Tissue and Cell 44 (2012) 401–408

Contents lists available at SciVerse ScienceDirect

Tissue and Cell

journal homepage: www.elsevier.com/locate/tice

In vivo and *in vitro Leishmania amazonensis* infection induces autophagy in macrophages

Larissa Tavares Cyrino[a], Alexandra Paiva Araújo[a], Paulo Pinto Joazeiro[b], Cristina Pontes Vicente[c], Selma Giorgio[a,*]

[a] Departamento de Biologia Animal, Instituto de Biologia, Universidade Estadual de Campinas, Caixa Postal 6109, Cep 13.083-970, Campinas, São Paulo, Brazil
[b] Departamento de Histologia e Embriologia, Instituto de Biologia, Universidade Estadual de Campinas, Campinas, São Paulo, Brazil
[c] Departamento de Biologia Estrutural e Funcional, Instituto de Biologia, Universidade Estadual de Campinas, Campinas, São Paulo, Brazil

ARTICLE INFO

Article history:
Received 17 May 2012
Received in revised form 13 July 2012
Accepted 2 August 2012
Available online 30 August 2012

Keywords:
Leishmania amazonensis
Macrophages
Autophagy
LC3II protein
Parasitophorous vacuole

ABSTRACT

Autophagy is the primary mechanism of degradation of cellular proteins and at least two functions can be attributed to this biological phenomenon: increased nutrient supply *via* recycling of the products of autophagy under nutrient starvation; and antimicrobial response involved in the innate immune system. Many microorganisms induce host cell autophagy and it has been proposed as a pathway by which parasites compete with the host cell for limited resources. In this report we provide evidence that the intracellular parasite *Leishmania amazonensis* induces autophagy in macrophages. Using western blotting, the LC3II protein, a marker of autophagosomes, was detected in cell cultures with a high infection index. Macrophages infected with *L. amazonensis* were examined by transmission electronic microscopy, which revealed enlarged myelin-like structures typical late autophagosome and autolysosome. Other evidence indicating autophagy was Lysotracker red dye uptake by the macrophages. Autophagy also occurs in the leishmaniasis skin lesions of BALB/c mice, detected by immunohistochemistry with anti-LC3II antibody. In this study, autophagy inhibitor 3-methyladenine (3MA) reduced the infection index, while autophagy inductors, such as rapamycin or starvation, did not alter the infection index in cultivated macrophages, suggesting that one aspect of the role of autophagy could be the provision of nutritive support to the parasite.

1. Introduction

Autophagy is the primary mechanism of degradation of cellular proteins and organelles, and involves the sequestration of regions of the cytosol within bound double-membrane that matures and degrades cytoplasmic constituents (Levine, 2007; Levine et al., 2011). At least two functions can be attributed to autophagy: increased nutrient supply *via* recycling of the products of autophagy under nutrient starvation, which is an important mechanism in maintaining cellular homeostasis (Levine et al., 2011; Mizushima, 2007); and autophagy could have an antimicrobial function and is involved in the innate immune response (Kirkegaard et al., 2004; Fabri et al., 2011), for example, in the removal of invading bacteria, including group A *Streptococcus* (Nakagawa et al., 2004), *Shigella* (Ogawa et al., 2005), and *Listeria* (Rich et al., 2003). However the relation between pathogens and autophagy appears to be complex. One example is the induction of host cell autophagy by the intracellular apicomplexa parasite *Toxoplasma gondii* (Wang et al., 2009a). It has also been suggested as a pathway by which parasite can compete with the host cell for limited resources (Wang et al., 2009b). *Chlamydia*, an obligate intracellular bacterium, induces autophagy that plays a defensive role in cells infected with chlamydial species not adapted to the host species. On the other hand, autophagy supports bacterial growth in permissive cells (Yasir et al., 2011). For *Leishmania*, an intracellular protozoan parasite that lives and proliferates within parasitophorous vacuoles (PV) of mononuclear phagocytes and causes a spectrum of human diseases (Kima, 2007; Nylén and Gautam, 2010; Mougneau et al., 2011), few reports exists of an association between the parasite and autophagy. One of the earliest reports suggested that *Leishmania mexicana* acquired macromolecules from the host cell *via* the mechanism of autophagy (Schaible et al., 1999). Pinheiro et al. (2009) showed that autophagy induction by starvation or cytokines alters parasite load, depending on the strain of mice used, while Mitroulis et al. (2009) detected autophagy in bone marrow taken from a patient with visceral leishmaniasis.

In this report, our group presents data demonstrating that *Leishmania amazonensis* infection induces autophagy in cultivated macrophages using three different methods; blot detection of

* Corresponding author. Tel.: +55 19 35216287; fax: +55 19 35216287.
E-mail address: sgiorgio@unicamp.br (S. Giorgio).

0040-8166/$ – see front matter © 2012 Elsevier Ltd. All rights reserved.
http://dx.doi.org/10.1016/j.tice.2012.08.003

LC3II, a marker of the autophagy pathway that is predominantly associated with autophagic organelles, transmission electron microscopy, and Lysotracker red staining (Klionsky et al., 2007). We also investigated whether autophagy modulation alters *in vitro L. amazonensis* infection. In addition, the occurrence of autophagy was examined in the cutaneous lesions of infected mice.

2. Materials and methods

2.1. Animals, parasite, and cell cultures

Female BALB/c and C57Bl/6 mice, aged 6–8 weeks, were obtained from Animal Center of the Campinas State University (Unicamp), Campinas, SP, Brazil. *L. amazonensis* (MHOM/BR/73/M2269) amastigotes were isolated from footpad lesions of BALB/c mice (Centro Multidisciplinar para Investigação Biológica, Unicamp) as described previously (Barbieri et al., 1993), and used immediately following isolation. Promastigotes were cultured as described by Arrais-Silva et al. (2005). The murine macrophage cell line RAW264.7 was maintained in RPMI 1640 medium supplemented with gentamicin with 25 μg/ml gentamicin (Sigma, St. Louis, MO, USA) and 10% fetal calf serum (FCS) (Nutricel, Campinas, SP, Brazil) at 37 °C in 5% CO_2, 5% O_2, and balanced N_2 (Linares et al., 2008). Bone marrow-derived macrophages (BMDM) were obtained from normal BALB/c or C57Bl/6 mice total bone marrow by flushing femurs and tibia with Dulbecco's modified Eagle's (DME) medium; the bone marrow mononuclear cells were propagated by culturing in DME medium supplemented with 10% FCS and 20% L929-conditioned medium for seven days (Swanson et al., 2009). The murine fibrosarcoma cell line L929 were cultured as described previously to generate L929-conditioned medium (Swanson et al., 2009). All the experimental protocols were approved by the Ethics Committee for Animal Research of the Institute of Biology, Unicamp.

2.2. Animal infection

Six-week-old female BALB/c mice were subcutaneously infected in the right hind footpad with 10^5 amastigotes. The course of the infection was monitored by measuring the increase in footpad thickness with a dial caliper compared with the contralateral uninfected footpad (Arrais-Silva et al., 2006).

2.3. Macrophage treatment and infection

For autophagy induction through starvation, cells were washed three times with PBS and incubated with Hanks balanced salt solution (Sigma) at 37 °C in 5% CO_2, 5% O_2, and balanced N_2; alternatively autophagy was induced by treatment with rapamycin 50 μg/ml in DME medium with 10% FCS (Singh et al., 2006). The specific inhibitor of autophagy used was 3-methyladenine (3MA) (Sigma) (Wang et al., 2009a). RAW and BMDM cells were infected with *L. amazonensis* amastigotes at different parasite–cell ratios for 1–24 h, as previously described (Colhone et al., 2004). Briefly, following a period of interaction, the cultures were washed to remove extracellular parasites and fresh medium was added to the cell cultures. To determine the percentage of infected macrophages and number of amastigotes per macrophage, cells on coverslips were stained with Giemsa and examined microscopically at 1000× magnification. At least 200 cells were counted per triplicate coverslip.

2.4. LC3II protein detection

Immunohistochemistry of LC3II in murine cutaneous lesions were performed using rabbit polyclonal anti-LC3 (Novus Biologicals, Littleton, CO, USA) developed with goat polyclonal anti-rabbit antibody conjugated with peroxidase (Sigma). Serial 5 μm thick paraffin sections of footpad were treated as follows: deparaffination, rehydration, endogenous quenching, and citrate buffer microwave retrieval and visualized with a peroxidase substrate solution containing 3,3′-diaminobenzidine and hydrogen peroxide, as previously described (Arrais-Silva et al., 2005; Araújo et al., 2010). The images were recovered with a digital imaging system, a light microscope (Eclipse E800, Nikon, Tokyo, Japan), a Cool Snap-Pro Color camera (Media Cybernetics, Bethesda, MD, USA) and capture software Image-Pro plus (Media Cybernetics). The LC3II were detected by immunoblotting in cultured macrophages. For immunochemical analyses of LC3II in macrophages cultured *in vitro*, cells were scraped from culture flasks, checked for viability, and then rinsed twice with PBS. Lysis buffer (62.5 mM Tris–HCl, pH 6.8, 69 mM SDS, 10% glycerol, 2% 2-mercaptoethanol, 34 mM ethylenediaminetetraacetic acid, 2 μg/ml pepstatin, and 1 mM phenylmethylsulfonyl fluoride; Amersham Pharmacia Biotech, Piscataway, NJ, USA) was added to the cell pellets. Proteins were denatured at 40 °C for 1 min, electrophoresed on tricine-SDS-PAGE and transferred to nitrocellulose membranes (Amersham Pharmacia Biotech). After blotting, membranes were blocked with 5% (w/v) nonfat dry milk for 1 h and incubated with rabbit polyclonal anti-LC3 (Novus Biologicals) or mouse anti-β actin (Sigma) overnight at 4 °C. The secondary antibodies consisted of peroxidase-conjugated anti-rabbit and mouse IgGs (Sigma Aldrich) and were developed with 3,3-diaminobenzidine (Degrossoli et al., 2004). Immunoreaction images were scanned and the densitometric value of each band was determined using Image Master Total Lab version 1 software (Amersham Pharmacia Biotech).

2.5. Ultrastructural analyses

The macrophages (2×10^5) were seeded in eight-well chamber slides (Permanox Lab Tek, Nunc, Naperville, IL, USA) and a fixative consisting of 2.5% glutaraldehyde (Electron Microscope Science, Hatfield, PA) in 0.1 M sodium cacodylate (Electron Microscope Science) buffer at pH 7.4 was added to the medium of adherent cells for 15 min. Then, the fixative and medium mixture was replaced by pure fixative for 45 min. Next, the cells were rinsed (3–10 min) in 0.1 M sodium cacodylate buffer, pH 7.4 and then post-fixed in 1% OsO_4 (Electron Microscope Science) solution for 1 h. Following dehydration in an ethanol gradient, adherent cells were embedded in Epon 812 resin (Electron Microscope Science). Ultrathin sections were stained with uranyl acetate and lead citrate and observed in a LEO 906 (Leica, Wetzlar, Germany) transmission electron microscope operated at 60 kV (Degrossoli et al., 2011).

2.6. Lysotracker red staining

Lysotracker (Lysotracker red, Lonza, Walkersville, MD, USA) was used in accordance with the manufacturer's instructions. Briefly, cells were stained with 100 nM Lysotracker red at 37 °C for 1 h. After washing three times with PBS, cells were immediately analyzed under phase-contrast and fluorescence using fluorescence inverted microscopy (Nikon-Eclipse TS100).

2.7. Statistical evaluation

All experiments were repeated at least three times and the results are expressed as the mean ± SD. Data obtained under different conditions were analyzed statistically by the Student *t* test for independent samples ($P \leq 0.01$).

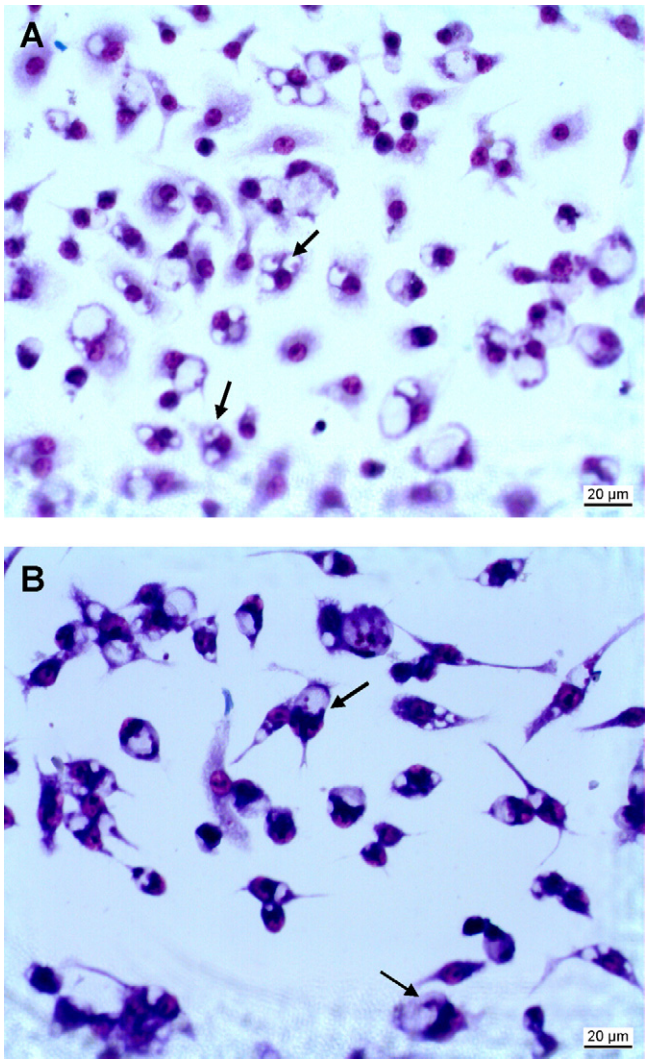

Fig. 1. Photomicrographs of macrophages infected with *L. amazonensis*. (A) BMDM culture was infected with amastigotes at a parasite–macrophage ratio of 3:1 for 24 h. (B) RAW culture was infected with amastigotes at a parasite–macrophage ratio of 10:1 for 16 h. Arrowheads indicate intracellular parasites inside PV.

3. Results

3.1. LC3II expression in cultured macrophages infected with L. amazonensis

To test whether *L. amazonensis* induces autophagy in host macrophages, cells were infected with amastigotes. As shown in Fig. 1 most BMDM and RAW macrophages in the cultures presented PV containing parasites, which are characteristics of *L. amazonensis* infection. The infection level in BMDM was around 70% and 3–4 amastigotes per cell and in RAW macrophages was around 60% and 3–4 amastigotes per cell. Next we evaluated the expression of LC3II, the lipidated form of LC3I and a marker of autophagy (Shintami and Klionsky, 2004; Klionsky et al., 2007). Fig. 2 shows that the amount of LC3II was increased following infection; while no or low levels of LC3II were detected in uninfected macrophages. The results were comparable using BMDM from BALB/c or C57Bl/6 mice and RAW macrophages (Figs. 2A and 1B), which were equally infected with *L. amazonensis* (Fig. 2C). Analysis of our results further showed that elevated levels of LC3II were associated with increased infection index (% of infected cells × number of the intracellular parasites); *i.e.*, more infection resulted in enhanced LC3II expression in macrophages (Fig. 3). The data suggest that *L. amazonensis* induces host macrophage autophagy.

3.2. Electron microscopy of cultured macrophages infected with L. amazonensis

Consistent with the findings showed above are the electronic microscopy results. We used electronic microscopy analyses because typical structures could be formed in the autophagic process (Singh et al., 2006). In fact, myelin-like structures suggesting autophagosome and autolysosome were observed in infected macrophages (Fig. 4C). Interestingly, parasites are never observed surrounded by these autophagosome- and autolysosome-like vesicles (Fig. 4C). Nutrient starvation triggered autophagy (Swanson et al., 2009) and typical double membrane vesicles containing residual material around macroautophagosomes were observed in starved macrophages, included as a positive control (Fig. 4B).

3.3. Lysotracker red staining of cultured macrophages infected with L. amazonensis

Lysotracker red, a dye that accumulates in acidic compartments (autophagosomes/lysosomes) (Klionsky et al., 2007) was tested in macrophages. As shown in Fig. 5, Lysotracker red accumulated in intracellular organelles (2 puncta per cell) but there was little or no staining in PV of macrophages infected with *L. amazonensis*. It should be noted that Lysotracker red stain was not observed in neighboring uninfected cells. As expected, Lysotracker puncta were observed in starved macrophages (2.25 puncta per cell) but not observed in uninfected control cells (0.4 puncta per cell) (Fig. 5). The data obtained from three different methods of detection revealed that *L. amazonensis* induces autophagy in host macrophages.

3.4. Induction of autophagy in cultured macrophages infected with L. amazonensis

The next step was to evaluate whether the macrophage autophagy had some impact on *L. amazonensis* infection. The starvation regime was used as inductor of autophagy in macrophages before infection (Fig. 6). As expected, LC3II levels were detected in starved cells (Biswas et al., 2008; Martinet et al., 2009 and Fig. 6) and in macrophages infected with *L. amazonensis* (Fig. 6). Interestingly, autophagy induced in macrophages by starvation and then infected with *L. amazonensis* produced higher levels of LC3II and an infection index comparable to that of nonstarved macrophages infected with the parasites (Fig. 6). We also used common autophagy inductors rapamycin and starvation and the autophagy inhibitor 3MA to evaluate the effect of RAW macrophage autophagy on *L. amazonensis*. As shown in Fig. 7, the starved RAW cells did not alter the infection index compared with nonstarved macrophages. Similar results were observed using rapamycin treatment to induce autophagy (Fig. 7). In contrast, 3MA treatment inhibited the infection index in RAW macrophages (Fig. 7). It should be noted that in contrast to typical amastigote morphology seen in cells treated with rapamycin and starved cells, many macrophages in the population treated with 3MA had clear their infection or had few parasites and disintegrate parasite fragments inside (data not shown).

3.5. LC3II expression in lesion of mice infected with L. amazonensis

To determine whether *L. amazonensis* infection induces autophagy *in vivo*, we used a mouse model of cutaneous leishmaniasis (Giorgio et al., 1998). The skin lesions of BALB/c mice increased rapidly, most of the mice presented footpad skin ulcers, metastatic skin lesions and died after 150 days (Giorgio et al., 1998).

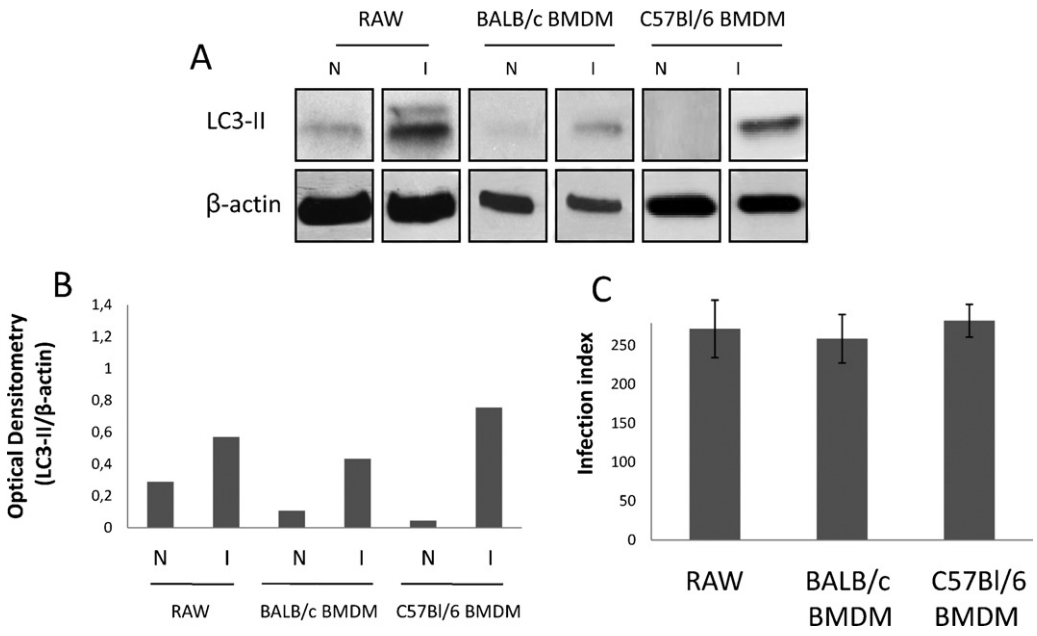

Fig. 2. Western blot analysis of LC3II and *L. amazonensis* infection in macrophages. (A) RAW macrophages non infected (N) and infected with *L. amazonensis* (I), BALB/c mice BMDM non infected (N) and infected with *L. amazonensis* (I), C57Bl/6 mice BMDM non infected (N) and infected with *L. amazonensis* (I). (B) Bars represent the results of LC3II to β-actin ratio as measured by densitometry. (C) BMDM and RAW macrophages were infected with amastigotes and cultured for 16 and 24 h respectively. The infection index was determined as described in Section 2. Results of a representative experiment out of five.

Paraffin-embedded lesions were examined by immunohistochemistry using anti-LC3II antibody (Fig. 8). Macrophages containing parasites within PV are found predominant cell (85–90%) in the skin lesions with inflammatory cells polymorphonuclear leukocytes and lymphocytes in small number (10–15%) (Fig. 8). We verified positive staining for LC3II in macrophages (38%) and inflammatory cells (3%) (Fig. 8B) and LC3II deposition was located in the cytoplasm at 70 days after infection. Later in the infection (150 days), lesions showed a similar histological pattern, but with greater numbers of heavily parasitized macrophages replacing the normal tissue (Fig. 8C and D). The LC3II positive macrophages (46%) were mixed with LC3II negative macrophages (42%) and inflammatory cells (2% LC3II positive cells) (Fig. 8C). It should be noted that LC3II was not detected in normal footpad (Fig. 8A). The data suggest that an autophagic phenomenon occurs in numerous macrophages infected with *L. amazonensis* present within skin lesions.

4. Discussion

In this study, we provide evidence that *L. amazonensis* infection induces autophagy in macrophages. The LC3II protein the marker of autophagosomes (Klionsky et al., 2007; Sato et al., 2007) was

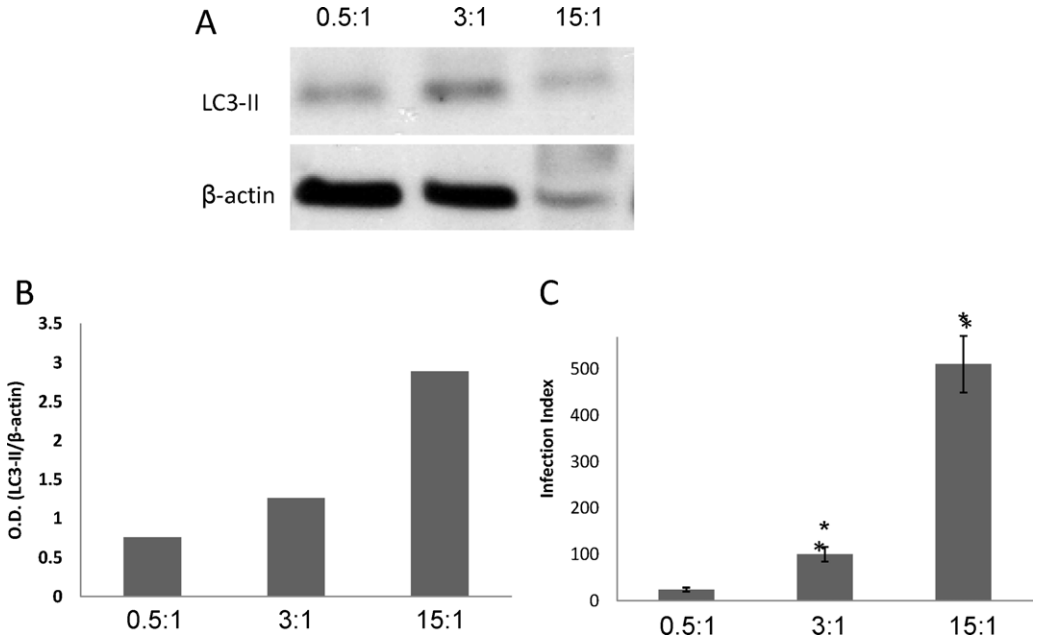

Fig. 3. Western blot analysis of LC3II and *L. amazonensis* infection in RAW macrophages. (A) RAW macrophages were infected with *L. amazonensis* at different parasite–cell ratio of 0.5:1, 3:1, and 15:1 for 1 h. (B) Bars represent the results of LC3II to β-actin ratio as measured by densitometry. (C) The infection index was determined as described in Section 2. Results of a representative experiment out of five.

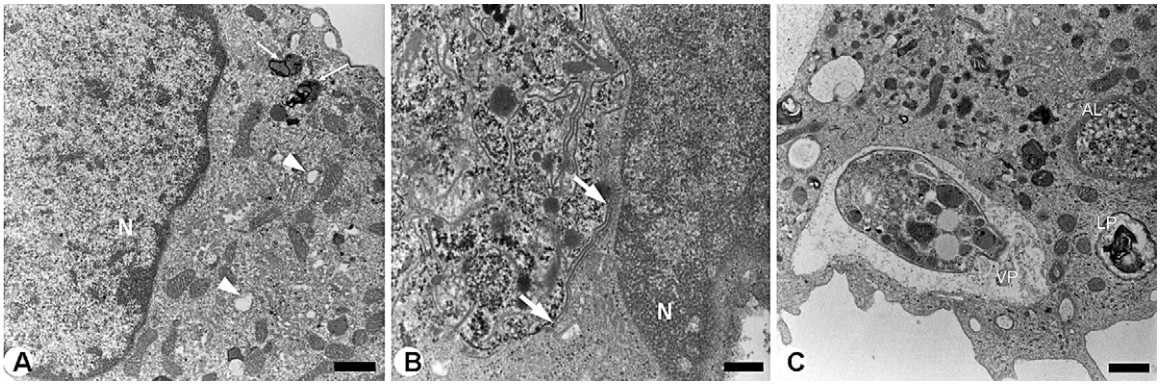

Fig. 4. Representative transmission electron micrographs of macrophages. (A) BALB/c mouse BMDM non infected cell showing well preserved nucleus (N), typical organelles, small vacuoles (arrow head), and lipid drop myelin-like microautophagosomes (thin arrow). (B) Starved BALB/c mouse BMDM macrophage with initial sequestration of cytosolic material containing ribosome-free ER sheet forming double membrane vesicle or phagopores (arrows) around a large area of cytoplasm typical of early stages in the biogenesis of macroautophagosomes. A part of the nucleus is seen at N. (C) BALB/c mouse BMDM infected with *L. amazonensis* amastigotes showing parasitophorous vacuole (PV) contained amastigotes, enlarged myelin-like structures typical late autophagosome (AP) and autolysosome (AL). Note that parasite or PV is not associated with any AP and AL. Bars: A and C, 800 nm; B, 300 nm.

detected by western blotting at high levels in cell cultures with a high infection index. The macrophages infected with *L. amazonensis* were examined by transmission electronic microscopy and contained multiple layered vesicles engulfing disrupted cell structures. Other evidence indicating autophagy during the infection was the Lysotracker red dye uptake by macrophages. These three methods have been used extensively to monitor autophagy in organs and cell systems (Klionsky et al., 2007). LC3 exist in two forms, as an unprocessed cytosolic protein (LC3I) and, following induction of autophagy, as a lipidated membrane-bound protein (LC3II) (Klionsky et al., 2007). Immunoblotting assay with antibody anti-LC3II detects the conversion of LC3I to LC3II and has been used to demonstrate autophagy in cell cultures, such as tumor cells (Shintami and Klionsky, 2004; Sato et al., 2007), macrophages infected with *Helicobacter pylori* (Wang et al., 2009b) and Hela cells infected with *T. gondii* (Wang et al., 2009a). Of some importance, Mitroulis et al. (2009) demonstrated autophagy in bone marrow macrophages from a patient

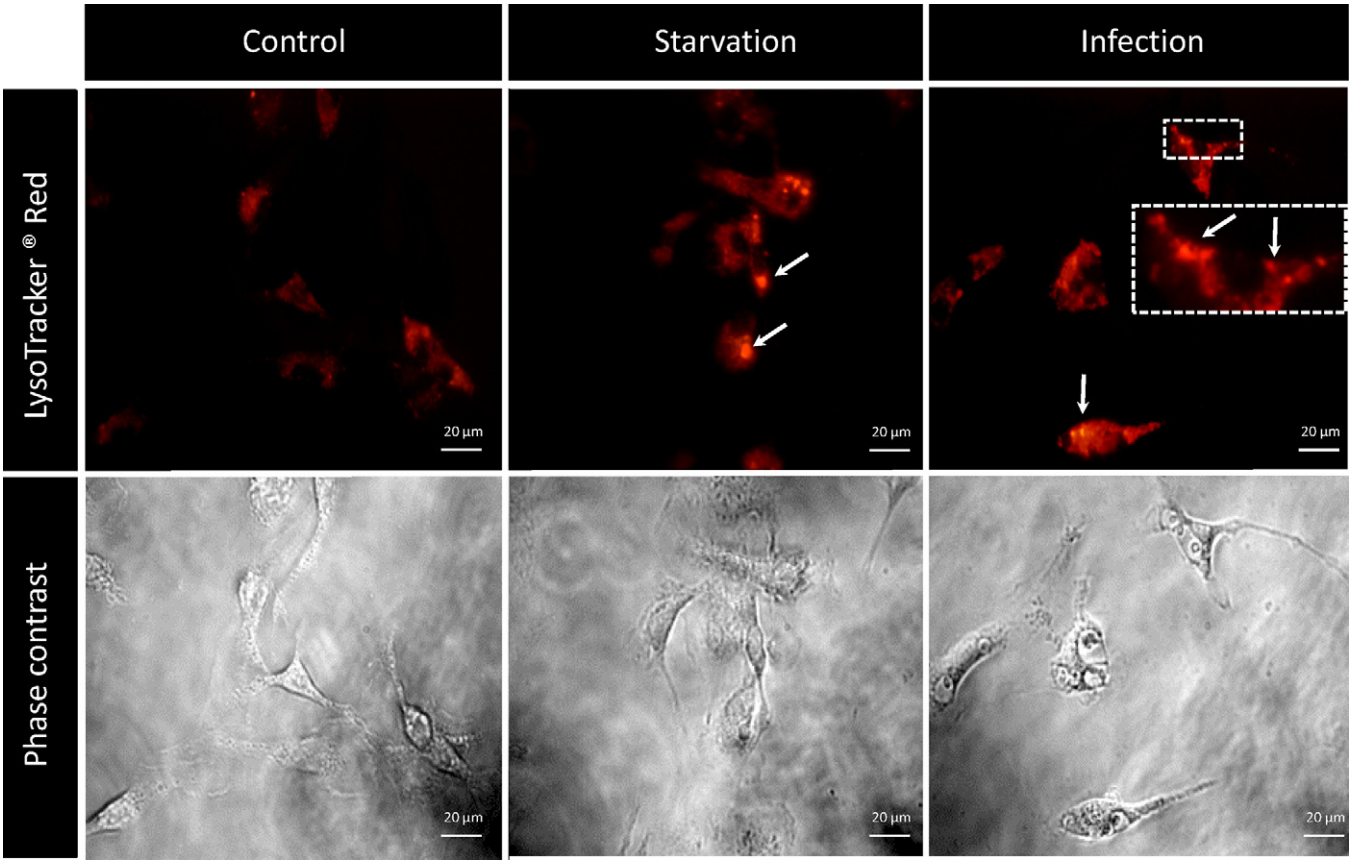

Fig. 5. Lysotracker red localization in macrophages. BMDM non infected (control), starved for 2 h or infected with *L. amazonensis* were incubated with Lysotracker red. Note stained acidic vesicles in starved macrophages. Macrophages infected with *L. amazonensis* showed fluorescence dispersed in the cytoplasm; amastigotes and PV are not stained. Phase-contrast microscopy of the same cultures show parasites and PV.

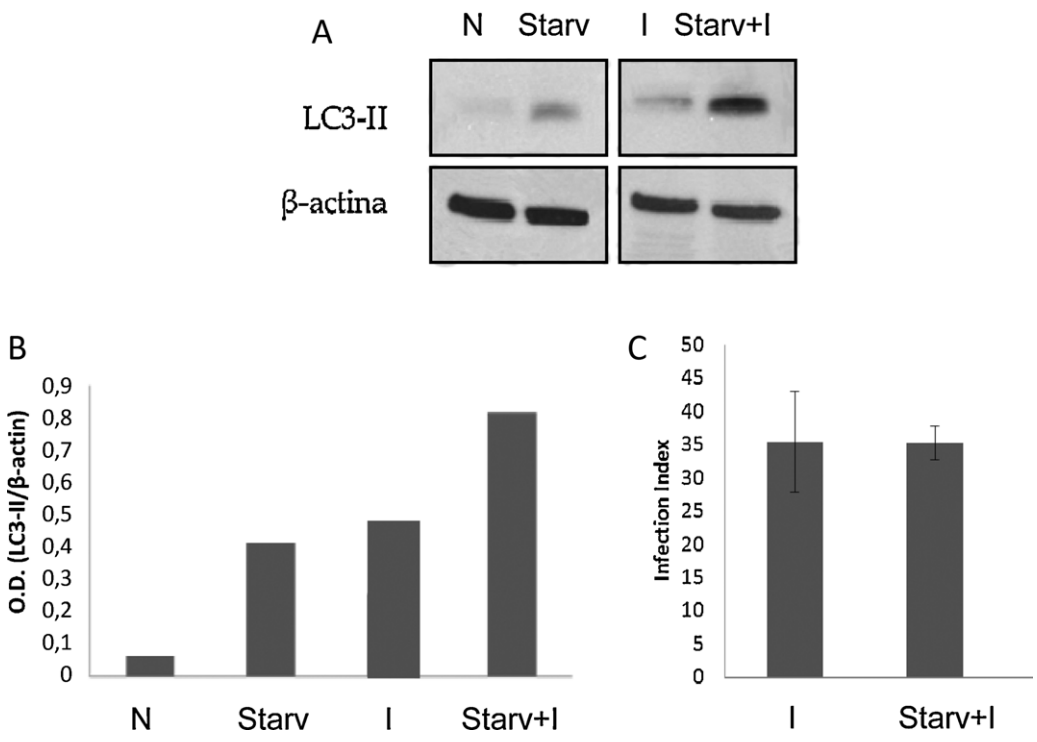

Fig. 6. Western blot analysis of LC3II and *L. amazonensis* infection in BMDM. (A) Macrophages non infected (N), starved for 2 h (starv), infected with *L. amazonensis* at a parasite–cell ratio of 3:1 for 24 h (I) or, starved for 2 h and then infected with *L. amazonensis* for 24 h (starv + I). (B) Bars represent the results of LC3II to β-actin ratio as measured by densitometry. (C) The infection index was determined as described in Section 2. Results of a representative experiment out of four.

infected with *L. donovani* using immunoblotting with anti-LC3II antibody. Electron microscopy was the earliest method to detect autophagy (Mitou et al., 2009) and the morphological signature is the formation of a crescent-shaped sliver of membrane within cytosol that wraps around cytoplasmic targets to form the autophagosome (Delgado et al., 2009), which was observed in macrophages treated with INF-γ (Singh et al., 2006) or infected with *H. pyroli* (Wang et al., 2009b). Schaible et al. (1999) demonstrated nascent autophagosomes in macrophages infected with *L. mexicana* and Pinheiro et al. (2009) observed myelin-like membrane in macrophages infected with *L. amazonensis* and treated with INF-γ. Similar to our results, the authors did not observe parasites inside the multilayer vesicles (Schaible et al., 1999). The third method the acid tropic dye Lysotracker red is frequently used following autophagy (Klionsky et al., 2007; Mitou et al., 2009). Although Lysotracker red is not a specific marker for autophagosomes because it also detects acidified endosomes and lysosomes (Klionsky et al., 2007; Mitou et al., 2009) the staining pattern of Lysotracker red in an indicative of autophagy. Lysotracker red-containing vesicles were observed in macrophages infected with *L. amazonensis*, although there is little or no staining by the dye in PV; suggesting that both autophagic compartments and PV can be discriminated in these macrophages. However, we cannot exclude the possibility that fusion occurs between the two organelles during infection. In fact, Schaible et al. (1999) observed that the transfer of fluorescent dextran into PV containing *L. mexicana* is sensitive to the autophagy inhibitor 3MA and suggested that degraded cytosolic material is delivered to PV.

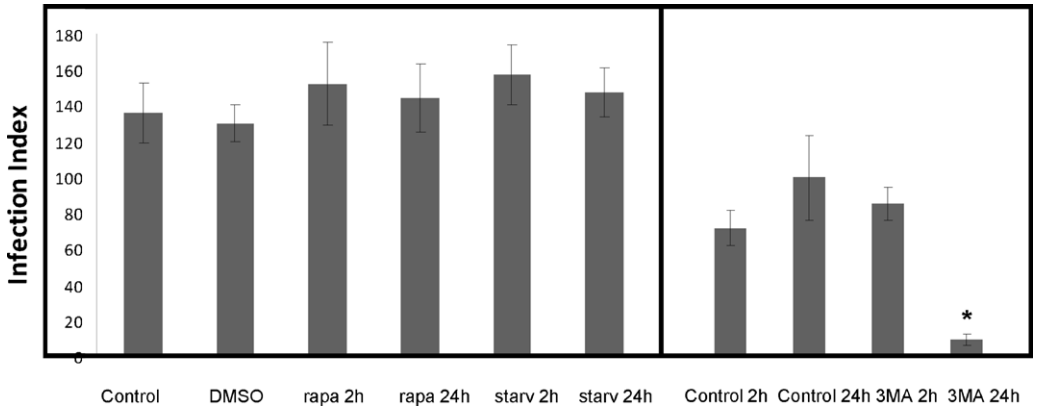

Fig. 7. The effect of rapamycin, starvation or 3MA in macrophages infected with *L. amazonensis*. RAW macrophages were infected with amastigotes at a parasite–cell ratio of 10:1 for 16 h and washed. As control cells were left untreated (control), treated with DMSO or rapamycin for 2 h (rapa 2 h) or 24 h (rapa 24 h), left in starvation for 2 h (starv 2 h) or 24 h (starv 24 h). RAW macrophages were infected with amastigotes at a parasite–macrophage ratio of 5:1 for 12 h and washed. As control cells were left untreated for 2 h (control 2 h) or 24 h (control 24 h), treated with 3MA for 2 h (3MA 2 h) or 24 h (3MA 24 h). Data are averages of three experiments, bars indicate SD. *Statistically significant difference relative to untreated cells ($P < 0.01$).

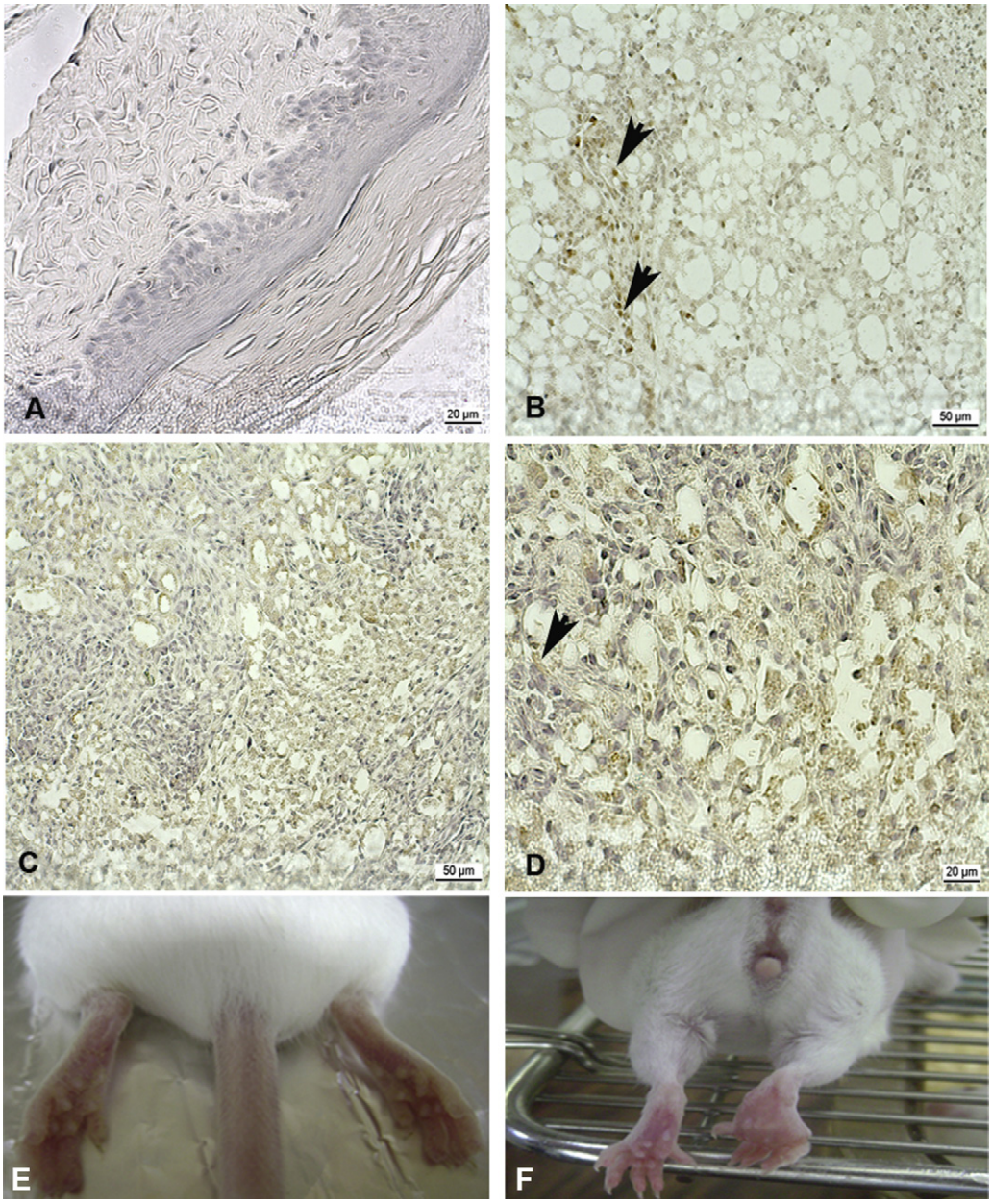

Fig. 8. Evaluation of autophagy in BALB/c mouse footpad tissues. (A) Normal mouse footpad tissue stained with anti-LC3II antibody and counterstained with hematoxylin. The top and bottom arrows indicate epidermis and dermis, respectively. No immunoreactivity was observed in the tissue. (B) Mouse footpad lesion at 70 days of *L. amazonensis* infection. The arrows indicate LC3II immunostaining in the cytoplasm of vacuolated and parasitized macrophages. (C) Mouse footpad lesion at 150 days of *L. amazonensis* infection. Note cellular population infiltrating the tissue with predominance of vacuolated and parasitized macrophages LC3II immunostained. (D) Higher magnification of mouse footpad lesion at 150 days of infection. The arrow indicates LC3II immunostaining of vacuolated and parasitized macrophages. Photographs of footpads of normal mouse (E) and mouse infected with 10^5 amastigotes 60 days earlier (F).

The question arises whether host macrophage autophagy is involved in the defense against *Leishmania* or has a pro-pathogen role. An inhibitory role of autophagy in pathogen growth was observed in *H. pylori* (Wang et al., 2009a), *Listeria* (Py et al., 2007), and *Mycobacterium tuberculosis* infections (Biswas et al., 2008). In contrast, pathogens like *T. gondii* (Wang et al., 2009b) hepatitis C virus (Ke and Chen, 2011) and *Coxiela* (Gutierrez et al., 2005) adapt to host cell autophagy, which may be needed to support the infection. 3MA an inhibitor of phosphoinositide 3-kinase which inhibit autophagy but also impairs phagocytosis (Harris et al., 2009) and autophagy stimulators such as rapamycin or starvation, are currently used to evaluate the effect of autophagy on the pathogens during infections (Pinheiro et al., 2009; Wang et al., 2009a). In this study, autophagy inhibition reduced the infection index, while autophagy induction did not alter the infection index in BMDM and RAW macrophages. Recently, Pinheiro et al. (2009) showed similar results with 3MA or wortmannin, another autophagy inhibitor; *i.e.*, a reduction in the parasite load in macrophages infected with *L. amazonensis* and treated with IFN-γ. The same authors showed that starvation or rapamycin treatment increased the parasite load in peritoneal macrophages of BALB/c mice, but not in peritoneal macrophages of C56Bl/6 mice. Jaramillo et al. (2011) showed that rapamycin treatment increased parasite load in murine peritoneal macrophages infected with *Leishmania major* promastigotes. The different results obtained by Pinheiro et al. (2009), Jaramillo et al. (2011), and our group regarding the effects of autophagy inductors on cells infected with *Leishmania* could be explained by the use of different macrophage types (inflammatory and non

inflammatory peritoneal macrophages, J774 and RAW cells and BMDM) and parasite forms and species (amastigotes and promastigotes; *L. amazonensis* and *L. major*). It should be noted that the amastigote is the obligate intracellular parasite form adapted for survival and growth inside PV. The reason that autophagy inductors do not alter the infection index in macrophages infected with amastigotes may well be that amastigote itself induces sufficient autophagy in the host macrophage to maintain high parasite growth. In fact, a role of autophagy could be providing nutritive support to the parasite (Wang et al., 2009b). This is also consistent with the observation that *L. mexicana* can acquire macromolecules from macrophage cytosol *via* autophagy (Schaible et al., 1999).

Our study also provided evidence that autophagy occurs in leishmaniasis skin lesions from BALB/c mice. LC3II immunohistochemistry staining used in the experiments has been validated as a surrogate marker of autophagy by evaluating numerous tumor lesions, including adenocarcinomas (Sato et al., 2007) and human tumor xenografts (Holt et al., 2011). Taken together this report represents a step toward understanding the role of autophagy induced by *Leishmania* and its relevance in disease progression.

Acknowledgments

This work was supported by Fundação de Amparo à Pesquisa do Estado de São Paulo and Conselho Nacional de Desenvolvimento Científico e Tecnológico.

References

Araújo, A.P., Frezza, T.F., Allegretti, S.M., Giorgio, S., 2010. Hypoxia, hypoxia-inducible factor-1α and vascular endothelial growth factor in a murine model of *Schistosoma mansoni* infection. Exp. Mol. Pathol. 89, 327–330.

Arrais-Silva, W.W., Colhone, M.C., Ayres, D.C., Souto, P.C.S., Giorgio, S., 2005. Effects of hyperbaric oxygen on *Leishmania amazonensis* promastigotes and amastigotes. Parasitol. Int. 54, 1–7.

Arrais-Silva, W.W., Pinto, E.F., Rossi-Bergmann, B., Giorgio, S., 2006. Hyperbaric oxygen therapy reduces the size of *Leishmania amazonensis*-induced soft tissue lesions in mice. Acta Trop. 98, 130–140.

Barbieri, C.L., Giorgio, S., Merjan, A.J., Figueiredo, E.N., 1993. Glycosphingolipid antigens of *Leishmania* (*Leishmania*) *amazonensis* amastigotes identified by use of a monoclonal antibody. Infect. Immun. 61, 2131–2140.

Biswas, D., Qureshi, O.S., Lee, W.Y., Croudace, J.E., Mura, M., Lammas, D.A., 2008. ATP-induced autophagy is associated with rapid killing of intracellular mycobacteria within human monocytes/macrophages. BioMed Central Immunol. 9, 35–40.

Colhone, M.C., Arrais-Silva, W.W., Picoli, C., Giorgio, S., 2004. Effect of hypoxia on macrophage infection by *Leishmania amazonensis*. J. Parasitol. 90, 510–520.

Degrossoli, A., Arrais-Silva, W.W., Colhone, M.C., Gadelha, F.R., Joazeiro, P.P., Giorgio, S., 2011. The influence of low oxygen on macrophage response to *Leishmania* infection. Scand. J. Immunol. 74, 165–170.

Degrossoli, A., Colhone, M.C., Arrais-Silva, W.W., Giorgio, S., 2004. Hypoxia modulates expression of the 70-kDa heat shock protein and reduces *Leishmania* infection in macrophages. J. Biomed. Sci. 11, 847–850.

Delgado, M., Singh, S., De Haro, S., Máster, S., Ponpuak, M., Dinkins, C., Ornatowski, W., Vergne, I., Deretic, V., 2009. Autophagy and pattern recognition receptors in innate immunity. Immunol. Rev. 227, 189–190.

Fabri, M., Realegeno, S.E., Jo, E.K., Modlin, R.L., 2011. Role of autophagy in the host response to microbial infection and potential for therapy. Curr. Opin. Immunol. 23, 65–70.

Giorgio, S., Linares, E., Ischiropoulos, H., Von Zuben, F.J., Yamada, A., Augusto, O., 1998. *In vivo* formation of electron paramagnetic resonance-detectable nitric oxide and nitrotyrosine is not impaired during murine leishmaniasis. Infect. Immun. 66, 807–810.

Gutierrez, M.G., Vázquez, C.L., Munafó, D.B., Zoppino, F.C., Berón, W., Rabinovitch, M., Colombo, M.I., 2005. Autophagy induction favours the generation and maturation of the Coxiella-replicative vacuoles. Cell. Microbiol. 7, 981–990.

Harris, J., Hanrahan, O., De Haro, S.A., 2009. Measuring autophagy in macrophages. Curr. Protoc. Immunol. 87, 14.14.1–14.14.13.

Holt, S.V., Wyspianska, B., Randall, K.J., James, D., Foster, J.R., Wilkinson, R.W., 2011. The development of an immunohistochemical method to detect the autophagy-associated protein LC3-II in human tumor xenografts. Toxicol. Pathol. 39, 516–520.

Jaramillo, M., Gomez, M.A., Larsson, O., Shio, M.T., Topisirovic, I., Contreras, I., Luxenburg, R., Rosenfeld, A., Colina, R., McMaster, R.W., Olivier, M., Costa-Mattioli, M., Sonenberg, N., 2011. *Leishmania* repression of host translation through mTOR cleavage is required for parasite survival and infection. Cell Host Microbe 21, 331–340.

Ke, P.Y., Chen, S.S., 2011. Activation of the unfolded protein response and autophagy after hepatitis C virus infection suppresses innate antiviral immunity *in vitro*. J. Clin. Invest. 121, 37–40.

Kima, P.E., 2007. The amastigote forms of *Leishmania* are experts at exploiting host cell processes to establish infection and persist. Int. J. Parasitol. 37, 1087–1090.

Kirkegaard, K., Taylor, M.P., Jackson, W.T., 2004. Cellular autophagy: surrender, avoidance and subversion by microorganisms. Nat. Rev. Microbiol. 2, 301–310.

Klionsky, D.J., Cuervo, A.M., Seglen, P.O., 2007. Methods for monitoring autophagy from yeast to human. Autophagy 3, 181–190.

Levine, B., 2007. Cell biology: autophagy and cancer. Nature 446, 745–750.

Levine, B., Mizushima, N., Virgun, H.W., 2011. Autophagy in immunity and inflammation. Nature 469, 323–330.

Linares, E., Giorgio, S., Augusto, O., 2008. Inhibition of *in vivo* leishmanicidal mechanisms by tempol: nitric oxide down-regulation and oxidant scavenging. Free Radic. Biol. Med. 44, 1668–1670.

Martinet, W., Schrijvers, D.M., Timmermans, J.P., Herman, A.G., De Meyer, G.R., 2009. Phagocytosis of bacteria is enhanced in macrophages undergoing nutrient deprivation. FEBS J. 276, 2227–2230.

Mitou, G., Budak, H., Gozuacik, D., 2009. Techniques to study autophagy in plants. Int. J. Plant Genomics 2009, 451357.

Mitroulis, I., Kourtzelis, I., Papadopoulos, V.P., Mimidis, K., Speletas, M., Ritis, K., 2009. *In vivo* induction of the autophagic machinery in human bone marrow cells during *Leishmania donovani* complex infection. Parasitol. Int. 58, 475–480.

Mizushima, N., 2007. Autophagy: process and functions. Genes Dev. 21, 2861–2870.

Mougneau, E., Bihl, F., Glaichenhaus, N., 2011. Cell biology and immunology of *Leishmania*. Immunol. Rev. 240, 286–290.

Nakagawa, I., Amano, A., Mizushima, N., Yamamoto, A., Yamaguchi, H., Kamimoto, T., Nara, A., Funao, J., Nakata, M., Tsuda, K., Hamada, S., Yoshimori, T., 2004. Autophagy defends cells against invading group A *Streptococcus*. Science 306, 1037–1040.

Nylén, S., Gautam, S., 2010. Immunological perspectives of leishmaniasis. J. Global Infect. Dis. 2, 135–140.

Ogawa, M., Yoshimori, T., Suzuki, T., Sagara, H., Mizushima, N., Sasakawa, C., 2005. Escape of intracellular *Shigella* from autophagy. Science 307, 727–730.

Pinheiro, R.O., Nunes, P.N., Pinheiro, C.S., Dàvila, H., Bozza, P.T., Takiya, C.M., Corte-Real, S., Freire-de-Lima, C.G., Dos Reis, G.A., 2009. Induction of autophagy correlates with increased parasite load of *Leishmania amazonensis* in BALB/c but not C57BL/6 macrophages. Microbes Infect. 11, 181–190.

Py, B.F., Lipinski, M.M., Yuan, J., 2007. Autophagy limits *Listeria monocytogenes* intracellular growth in the early phase of primary infection. Autophagy 3, 117–120.

Rich, K.A., Burkett, C., Webster, P., 2003. Cytoplasmic bacteria can be targets for autophagy. Cell. Microbiol. 5, 455–460.

Sato, K., Tsuchihara, K., Fujii, S., Sugiyama, M., Goya, T., Atomi, Y., Ueno, T., Ochiai, A., Esumi, H., 2007. Autophagy is activated in colorectal cancer cells and contributes to the tolerance to nutrient deprivation. Cancer Res. 67, 9677–9680.

Schaible, U.E., Schlesinger, P.H., Steinberg, T.H., Mangel, W.F., Kobayashi, T., Russell, D.G., 1999. Parasitophorous vacuoles of *Leishmania mexicana* acquire macromolecules from the host cell cytosol via two independent routes. J. Cell Sci. 112, 681–690.

Shintami, T., Klionsky, D.J., 2004. Autophagy in health and disease: a double-edged sword. Science 306, 990–1000.

Singh, S.B., Davis, A.S., Taylor, G.A., Deretic, V., 2006. Human IRGM induces autophagy to eliminate intracellular mycobacteria. Science 313, 1438–1440.

Swanson, M.S., Byrne, B.G., Dubuisson, J.F., 2009. Kinetic analysis of autophagosome formation and turnover in primary mouse macrophages. Methods Enzymol. 452, 1–18.

Wang, Y., Weiss, L.M., Orlofsky, A., 2009a. Host cell autophagy is induced by *Toxoplasma gondii* and contributes to parasite growth. J. Biol. Chem. 284, 1694–1700.

Wang, Y.H., Wu, J.J., Lei, H.Y., 2009b. The autophagic induction in *Helicobacter pylori*-infected macrophage. Exp. Biol. Med. (Maywood) 234, 171–180.

Yasir, M., Pachikara, N.D., Bao, X., Pan, Z.K., Fan, H., 2011. Regulation of chlamydial infection by host autophagy and vacuolar ATPase-bearing organelles. Infect. Immun. 79, 4019–4020.